$^3P_1$-Orientation Velocity-Changing Collision Kernels Studied by Isolated Multipole Echoes

A. P. Ghosh, C. D. Nabors, M. A. Attili, and J. E. Thomas
Spectroscopy Laboratory and Physics Department, Massachusetts Institute of Technology, Cambridge, Massachusetts 02139
(Received 6 December 1984)

We report studies of ^{174}Yb $^3P_1$-orientation velocity-changing kernels with resolution sufficient to observe both classical and wave mechanical features. The measurements employ photon-echo techniques in which the echo intensity depends on the square of an isolated $J=1$ multipole moment for which the velocity-changing kernel is diagonal.

PACS numbers: 34.40.+n, 32.80.−t, 34.50.Fa, 34.90.+q

We report studies of $^3P_1$-orientation velocity-changing kernels for ^{174}Yb–rare-gas collisions with resolution sufficient to observe both classical and wave mechanical features. These are the first measurements which clearly resolve an anisotropic moment collision kernel, and are facilitated because the $^3P_1$ orientation is studied as an *isolated multipole* which evolves in velocity space as an independent entity.[1-3] The experiments achieve very high velocity resolution by employing photon-echo techniques in which the echo intensity is proportional to the square of a specific isolated multipole moment, and they permit each collision kernel to be studied by measuring a time-dependent decay rate.[4,5] In this way, $^3P_1$ isolated-multipole kernels are studied as conveniently as the $^1S_0 \rightarrow {}^3P_1$ optical dipole moment investigated previously.[6]

Isolated multipoles are studied by selection and measurement of velocities along the quantization ($\hat{\mathbf{z}}$) axis, about which the collision problem in the laboratory frame has cylindrical symmetry. Total angular momentum and parity conservation then require that the one-dimensional velocity-changing collision *kernels* for the $^3P_1$ orientation, $\rho_0^1(v_z)$, and transverse alignment, $\rho_2^2(v_z)$, be diagonal and real,[1,3] so that these moments are decoupled from other $J=1$ multipoles for which the kernels are not diagonal.

Isolated-multipole echo techniques are an extension of the stimulated (three pulse) echo techniques employed previously to study atomic velocity-changing collision kernels.[7,8] The experiments of Ref. 7 measured the decay of velocity-space gratings created in the Na population in order to study population collision kernels. Reference 8 studied Yb $^3P_1$ population kernels and also obtained information on the difference of the population and alignment kernels; two sets of measurements were required for data interpretation and low velocity resolution was achieved, compared to the present work.

In the isolated-multipole echo scheme (Fig. 1), a velocity grating is created in anisotropic moments of the ^{174}Yb $^3P_1$ excited state, by use of two suitably polarized ($\hat{\mathbf{e}}$) preparation pulses which are separated by a time delay T_g, and which propagate in the $\hat{\mathbf{z}}$ direction, resonant with the $^1S_0 \rightarrow {}^3P_1$ transition at 556 nm. This creates a velocity grating $\propto \cos(kv_zT_g)$ where k is the optical wave vector, and v_z the Yb z velocity. As shown below, by measurement of the decay rate of this grating for various T_g, *isolated anisotropic moment collision kernels* can be determined. In order to measure this decay rate with high resolution, a third $\hat{\mathbf{x}}$-polarized pulse is applied at a time T_3 to induce photon echo formation, and the polarization-rotated component ($\hat{\mathbf{y}}$) of the resulting stimulated echo is monitored. The stimulated echo intensity behind the blocking polarizer depends on the square of the anisotropic moment grating amplitude just prior to the third $\hat{\mathbf{x}}$ pulse.[1,4] Hence, the required decay rates are determined by measurement of the echo amplitude versus T_3, for fixed perturber pressure and fixed T_g, as is done in our experiments.

In general, the coupled amplitude equations for the $J=0, M=0$ and $J=1, M=\pm 1$ states can be solved and used to determine the field behind the blocking polarizer ($\hat{\mathbf{y}}$) just after the third ($\hat{\mathbf{x}}$) pulse, in terms of the amplitudes just prior to the $\hat{\mathbf{x}}$ pulse at time T_3. This field contains optical polarization terms which rephase at a time T_g relative to the third pulse (stimulated echo) and which depend on either of two anisotropic moments[9]: (i) the orientation $\rho_0^1(v_z, T_3)$ when a grating is prepared in the population difference

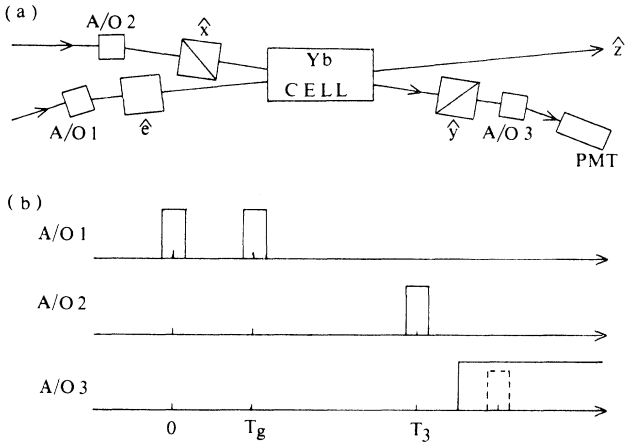

FIG. 1. (a) Isolated-multipole echo scheme. (b) Timing diagram.

between the $M=\pm 1$ states or (ii) the imaginary part of the transverse alignment, $\mathrm{Im}\rho_2^2(v_z,T_3)$, when a grating is prepared in the coherence between the $M=\pm 1$ states. As in Ref. 1 by choice of the preparation pulses as $\hat{\mathbf{e}}=\hat{\sigma}_+$, no transverse alignment is produced and the orientation is studied; for $\hat{\mathbf{e}}=(\hat{\mathbf{x}}+\hat{\mathbf{y}})/\sqrt{2}$ no orientation is produced and the transverse alignment is studied.

Our experiments employ velocity-selective excitation[1,6] so that the active-atom initial velocity v_z' is much smaller than that of the perturber for the small-angle collisions and time scales of these experiments.[1] In this case, the diagonal, real kernels are symmetric functions of the velocity change $\Delta v_z=v_z-v_z'$ and the collisional evolution equation determines that a velocity grating $\propto\cos(kv_zT_g)$ created in the selected moment decays exponentially at a rate[1,4,5]

$$\Gamma_q^k(T_g)=\gamma_q^k+\int_{-\infty}^{\infty}d(\Delta v_z)[1-\exp(ik\Delta v_zT_g)]\,W_q^k(\Delta v_z), \quad (1)$$

where $k,q=1,0$ for the orientation and 2,2 for the transverse alignment, γ_q^k is the destruction rate (analogous to the usual depolarization rate), and W_q^k is the one-dimensional kernel. During the time T between the second preparation pulse and the $\hat{\mathbf{x}}$ third pulse, the stimulated echo intensity decays by a factor $\exp[-2\Gamma_q^k(T_g)T]$, and so determines $\Gamma_q^k(T_g)$. Note that diffractive optical-polarization velocity-changing collisions[6] are significant for the long grating periods T_g employed in our experiments. However, these alter the grating contrast and the echo amplitude by a constant factor for fixed T_g and fixed perturber pressure, so that only $\Gamma_q^k(T_g)$ is measured when T is varied.

In the experiments (Fig. 1) acousto-optic intensity modulation of cw dye-laser (CR 599-21) radiation (~ 4 mW) is employed for pulse generation.[6] A small angle (1–2 mrad) between the preparation (A/O No. 1) and $\hat{\mathbf{x}}$-polarized (A/O No. 2) beams is used to eliminate background leakage (0.1–0.2 μW) from A/O No. 1 as well as to aid in the distinguishing of two pulse echoes. A/O No. 3 protects the photomultiplier from scattered preparation-pulse light. The Yb vapor-cell absorption is ~ 30–40% at 350 °C. The cell is placed in Helmholtz coils and shielded with two concentric cylinders of Mumetal maintained at a temperature 380 °C well below the Curie point (417 °C). This reduces transverse magnetic fields to a few milligauss, as measured with a three-axis Hall probe at room temperature. With the laser detuned from the Yb absorption, the $\hat{\mathbf{y}}$ polarizer is crossed with respect to the third-pulse ($\hat{\mathbf{x}}$) polarization. With the laser tuned to resonance small axial magnetic fields (due to counterwound oven heater imperfections) are then eliminated by adjustment of the Helmholtz z-axis field, using $\hat{\mathbf{x}}$-polarized preparation pulses and noting where the stimulated echo signal disappears. This procedure is checked for both short and long grating periods with and without rare-gas buffer. Pressure measurements are made with an MKS capacitance manometer (Model 310, 1-torr range).

For the orientation echo, which is studied in this Letter, a quarter-wave plate is inserted in the preparation pulse beam to obtain $\hat{\sigma}_+$ polarization. Results of measurements for Xe perturbers are shown in Fig. 2.

The orientation data are analyzed, in a first approximation, in two parts: (i) For small T_g, $k\Delta v_zT_g\sim 2\pi$ only for classical small-angle velocity changes. In this region, the kernel is calculated with use of a classical small-angle differential cross section which includes a survival probability taken to depend on impact parameter b as $\exp[-(b_i/b)^{10}]$, where b_i is the inelastic radius.[10] This differential cross section is similar to that of Ref. 8. (ii) For large T_g, $k\Delta v_zT_g\sim 2\pi$ for long-range diffractive velocity changes, and $\Gamma_0'(T_g)$ tends to the total collision rate γ_T for the $^3P_1$ state. A Gaussian differential cross section for the scalar van der Waals potential is used in the kernel.[11] The orientation grating decay, $\exp[-2\Gamma_0'(T_g)T]$, need not be averaged over initial velocity v_z' which is 0 for our velocity-selective excitation. However, the decay rate $\Gamma_0'(T_g)$ is only weakly dependent on v_z because of the perturber and active-atom velocity averages which appear in the one-dimensional kernel. To simplify analysis, $\Gamma_0'(T_g)$ is replaced by its thermal average over v_z', so that the three-dimensional kernel contains an isotropic average over atom-perturber relative speed v_r. The orientation decay rates obtained from

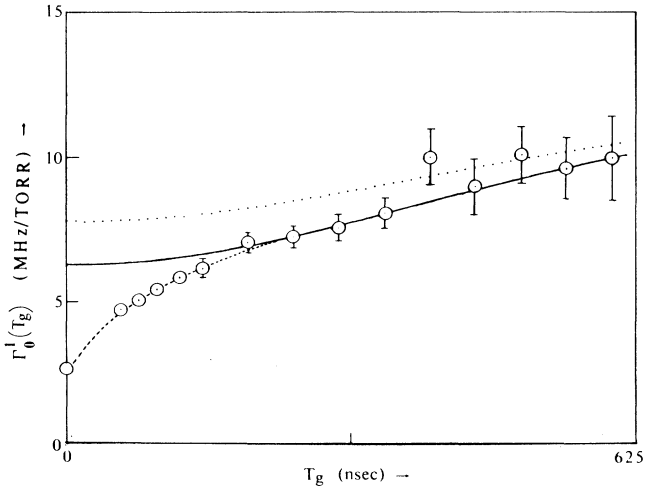

FIG. 2. Orientation time-dependent decay rate for Xe perturbers at 350 °C.

the corresponding one-dimensional kernels are then given by Eq. (1) in the approximate form[12]

$$\Gamma_0'(T_g) \simeq \gamma_0' + \frac{\gamma_0'}{3.48}\int_0^\infty dy\, y^{-7/3} e^{-y^{5/3}}\left[y - \frac{\sin\beta_1 y}{\beta_1}\right] \quad (2)$$

for small T_g and

$$\Gamma_0'(T_g) \simeq \gamma_T - \gamma_v \int_0^\infty 2dy \exp(-y^2)\frac{\sin\beta_2 y}{\beta_2} \quad (3)$$

for large T_g, where $\beta_1 = 0.28\delta v(\gamma_T/\gamma_0')^3 q T_g$ and $\beta_2 = 0.71\delta v q T_g$ with δv the diffractive velocity change, $2\hbar/mb_{el}$ (M = Yb mass), and q the optical wave vector. In terms of b_{el}, the relative velocity-averaged $^3P_1$ total collision rate is $\gamma_T = 7.95 N_p U_\mu b_{el}^2$ where N_p is the perturber density, and $U_\mu = (2kT/\mu)^{1/2}$ with μ the atom-perturber reduced mass.

The dashed curve of Fig. 2 shows the short-T_g fit using γ_0' obtained as in Ref. 1 and varying γ_T as the only free parameter. For the long-T_g data, the upper curve shows the fit for $\gamma_v = 0.37\gamma_T$, predicted for the extreme diffraction limit,[11,12] with γ_T from the short-T_g fit. The solid curve shows the fit for $\gamma_v = 0.50\gamma_T$.

Table I gives the results of the analysis for He, Ar, and Xe perturbers. The total cross sections obtained for Xe and Ar perturbers are in nearly the same ratio, 1.4, as that obtained for Yb optical radiators,[6] consistent with a van der Waals potential,[14] and in reasonable ($\sim 10\%$) agreement with the results of Ref. 8. The orientation decay rate γ_0', obtained by the method of Ref. 1, is substantially smaller than the alignment decay rate of Ref. 8 for Xe and comparable for He. Since the rank-one and -two decay rates are expected to be in the ratio 1.12:1[15] for van der Waals forces, the Xe results are inconsistent. The diffractive kernel fits the rare-gas data satisfactorily with use of a Gaussian distribution with the width expected for a van der Waals (C_6) potential[11] provided that the diffractive velocity changing rate γ_v is $0.5\gamma_T$ instead of $0.37\gamma_T$ expected for a C_6 force.[11]

The simplified analysis presented here focuses primarily on the $\Delta M = 0$ part of the orientation kernel. This kernel differs from that of the population, as studied in Ref. 8, in that the orientation is destroyed for close encounters, leading to $\Gamma_0'(T_g \to 0) \to \gamma_0'$ instead of $\Gamma_0'(T_g \to 0) = 0$. Hence, it is not surprising that the time-dependent decay rate for the orientation differs strongly from that of a population in the short-T_g region. Similar results are found in recent studies of the $M = 0, 1$ coherence kernels.[16]

However, other features expected for the orientation kernel are neglected in the present analysis. Generally, the one-dimensional kernel for the orientation can be written in laboratory magnetic state representation as $W_0'(\Delta v_z) = W_{+\leftarrow +}(\Delta v_z) - W_{-\leftarrow +}(\Delta v_z)$, where the first term is the M-conserving ($\Delta M = 0$) part while the second (negative) term is due to $\Delta M = 2$ collisions which flip the orientation. Physically, this latter process corresponds to the z component of the $^3P_1$ magnetic moment arriving inverted in the new velocity group. Our simplified analysis neglects this contribution. These processes, as well as a systematic study of the transverse alignment kernel, will be investigated in future work. Planned improvements in the spectrometer should permit more detailed study of the isolated-moment kernels, including direct inversion of the measured decay rate $\Gamma_q^k(T_g)$ by Fourier transformation, which according to Eq. (1) determines the complete isolated kernel.

TABLE I. Collision cross sections ($T = 350\,^\circ$C) (Ref. 13).

	σ_T (Å^2)	σ_0' (Å^2)
Xe	1107 ± 45	230 ± 14
Ar	789 ± 89	155 ± 18
He	258 ± 16	87 ± 5

We are grateful to T. W. Mossberg for stimulating discussion and to M. S. Feld for his enthusiastic support and encouragement in this work. This work was supported in part by the Massachusetts Institute of Technology Laser Research Center and by the U.S. National Science Foundation through Grant No. PHY-8315775.

[1]A. P. Ghosh, C. D. Nabors, M. A. Attili, J. E. Thomas, and M. S. Feld, Phys. Rev. Lett. **53**, 1333 (1984).

[2]J. E. Thomas, A. P. Ghosh, C. D. Nabors, M. Attili, R. A. Forber, and M. S. Feld, in *Proceedings of the Thirteenth International Quantum Electronics Conference Technical Digest, Anaheim, California, 1984* (IEEE, New York, 1984), p. 68.

[3]J. E. Thomas, to be published.

[4]See M. A. Attili, M. S. thesis, Massachusetts Institute of Technology, 1984 (unpublished).

[5]See C. D. Nabors, B. S. thesis, Massachusetts Institute of Technology, 1984 (unpublished).

[6]R. A. Forber, L. Spinelli, J. E. Thomas, and M. S. Feld, Phys. Rev. Lett. **50**, 331 (1983).

[7]T. Mossberg, A. Flusberg, R. Kachru, and S. R. Hartmann, Phys. Rev. Lett. **42**, 1665 (1979).

[8]See J.-L. Le Gouet and J.-C. Keller, in Proceedings of the Seventh International Conference on Spectral Line Shapes, Aussois, France, June 1984 (to be published); J.-C. Keller and J.-L. Le Gouet, Phys. Rev. Lett. **52**, 2034 (1984); J.-C. Keller and J.-L. Le Gouet, in Ref. 2; J.-C. Keller and J.-L. Le Gouet, Phys. Rev. A (to be published).

[9]Note that additional two-pulse echo-rephasing terms

which depend on the optical polarization can be distinguished by their rephasing time and their propagation direction, by use of a small angle between preparation and reading beams. See I. D. Abella, N. A. Kurnit, and S. R. Hartmann, Phys. Rev. **141**, 391 (1966).

[10]This approximation is similar to that used by A. Omont, J. Phys. (Paris) **26**, 26 (1965).

[11]See M. S. Child, *Molecular Collision Theory* (Academic, New York, 1974).

[12]For a more complete discussion see A. P. Ghosh *et al.*, to be published.

[13]Note that the cross sections are related to the rates according to $\gamma = N_p(2/\sqrt{\pi})U_\mu\sigma$, where U_μ is defined in the text.

[14]The use of the van der Waals C_6 potential to interpret long-range collision data for the heavier rare-gas perturbers obtained by photon-echo techniques has been used previously. See Ref. 8 and, for example, M. R. Woodworth, Opt. Lett. **8**, 307 (1983), and references therein.

[15]P. R. Berman and W. E. Lamb, Jr., Phys. Rev. **187**, 221 (1969).

[16]T. W. Mossberg, private communication.